

# Heralding of telecommunication photon pairs with a superconducting single photon detector

Martin A. Jaspan<sup>a)</sup>

Quantum Imaging Laboratory, Department of Electrical and Computer Engineering,  
Boston University, 8 Saint Mary's Street, Boston, Massachusetts 02215

Jonathan L. Habif

BBN Technologies, 10 Moulton Street, Cambridge, Massachusetts 02138

Robert H. Hadfield and Sae Woo Nam

National Institute of Standards and Technology, 325 Broadway, Boulder, Colorado 80305

(Received 11 January 2006; accepted 20 May 2006; published online 19 July 2006)

Experiments involving entangled photon pairs created via spontaneous parametric down conversion typically use wavelengths in the visible regime. The extension of a photonic quantum information link to a fiber optical network requires that entangled pairs be created at telecommunication wavelengths (1550 nm), for which photon counting detector technology is inferior to visible detection, in particular, low coincidence detection rates of correlated-photon pairs. We demonstrate a correlated-photon pair measurement using the superconducting single photon detector in a *heralding scheme* that can be used to substantially improve the correlated-photon detection rate.

© 2006 American Institute of Physics. [DOI: 10.1063/1.2219411]

The production and detection of entangled photon pairs has become a standard experiment in the field of quantum optics and has led to dramatic demonstrations of nonlocality in quantum mechanics. A growing area of research coordinates the entanglement physics with the field of information theory to perform communication and cryptographic tasks that have been impossible with classical media of information.<sup>1</sup>

Laboratory demonstrations of communication protocols that capitalize on the principles of quantum mechanics, such as quantum key distribution, have been tailored for use in modern communications systems using common telecommunication components.<sup>2</sup> Many experiments exploiting the physical properties of entanglement are incompatible with modern fiber optic networks, however, because the wavelengths typically used for downconverted photons are in the visible rather than the near infrared band, typical of fiber optic communications systems. The primary challenge of a near infrared (NIR) implementation is the lack of detector technologies for detecting single NIR photons reliably. Compared with silicon avalanche photodiode (APD) single photon detectors that detect visible wavelength photons, InGaAs/InP photodetectors<sup>3</sup> that are typically used for NIR photon counting have difficult commercial availability, low detection efficiency ( $\eta=10$  to 20%), high dark counts ( $P_d=10^4$  to  $10^5$  Hz) and slow relaxation rates (20–100  $\mu$ s), limiting them to clock speeds in the few megahertz range.<sup>4</sup> Using standard telecommunication components and InGaAs single photon detectors (SPDs) yield an inefficient way of producing and detecting NIR entangled photon pairs.<sup>5</sup> The long dead time blanking required to suppress afterpulsing substantially limits the achievable coincidence detection rates between pairs of detectors. Improvement of detector dark count rate and speed can drastically improve the overall throughput of an entangled source communication system rate of detection from an entangled source.

Two types of superconducting SPD (SSPD), the transition edge sensor (TES) and the NbN meander SSPD, have emerged as possible improvements over avalanche photodiodes. The TES has high  $\eta$ , low  $P_d$ , and is photon-number resolving but suffers from operation speeds in the kilohertz range and operates at  $\sim 100$  mK.<sup>6</sup> The SSPD in contrast can operate at 4 K, a temperature accessible with commercial cryogen-free refrigerators.<sup>7</sup> The SSPD is a nanoscale superconducting wire that is biased close to its critical current ( $I_c$ ). A photon striking the wire forms a hot spot causing a transient voltage over the device that is registered as a photon detection. The SSPD has low detection efficiency<sup>8,9</sup> (1%–20%) but low dark count rates and ability to operate with sources producing photons at gigahertz speeds.<sup>10,11</sup> Moreover, due to the low dark count rates and short dead times, the SSPD can be operated without gating electronics, as is necessary for the InGaAs APD, which makes it useful for implementing a heralded single photon source in the NIR.

The laboratory configuration for producing and detecting correlated 1550-nm photon pairs is shown in Fig. 1. A 775-nm Ti:sapphire laser, operating with 10-ps pulses at 80-MHz rate, pumps a spontaneous parametric downconverting (SPDC) source consisting of two 19-mm-long, type 1 periodically poled lithium niobate (PPLN) nonlinear crystals at 135 °C and with poling period 18.6  $\mu$ m. The geometry is

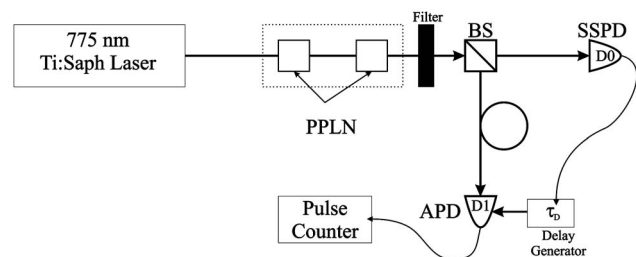


FIG. 1. Laboratory setup for producing wavelength degenerate correlated-photon pairs at 1550 nm. Pump laser aligned for type I phase matching through two 19-mm PPLN downconverting crystals. The correlated pairs are sent through a nonpolarizing beam splitter for coincidence detection.

<sup>a)</sup>Electronic mail: mjaspan@bu.edu

arranged for type I collinear degenerate phase matching, which has an extremely broad spectral output. A spectral filter ( $\Delta\lambda=10$  nm) is placed prior to collection of the collinear photon pairs into single-mode fiber and sent to a polarization insensitive beam splitter and with probability 1/2 directed toward separate SPDs, labeled D0 and D1 in Fig. 1.

The probability of a detector photoresponse, a *click*, is well approximated by  $P_{\text{click}}(i)=\mu\eta_i+P_d(i)$ , since both the photon probability times the detection efficiency and the detector dark count probability are small enough that higher-order products are neglected, and where  $i \in [D0, D1]$  is the detector index. The parameter  $\mu$  is used to describe the mean number of photon pairs generated per time bin.<sup>17</sup>

A coincidence event is recorded when both detectors click simultaneously; correlated coincidences due to detection of photon pairs occur with probability  $P_{\text{coinc}}=(\mu/2) \times (\eta_{D0}\eta_{D1})$ , the factor of  $\frac{1}{2}$  due to the splitting of degenerate photon pairs with a beam splitter, as compared to deterministic splitting of nondegenerate pairs, and *accidental* coincidences, due to uncorrelated detections and dark counts occur with probability  $P_{\text{acc}}=P_{\text{click}}(D0)P_{\text{click}}(D1)$ , the product of the individual probabilities for independent point processes.

Detector dead time can substantially limit the overall detection coincidence rate. Neglecting detector dead time, the detection coincidence rate is  $R_{\text{coinc}}=\frac{1}{2}f\mu(\eta_{D0}\eta_{D1})$ , where  $f$  is the system clock rate, the optical pulse rate. For a single detector, the dead-time-reduced click rate is approximately  $R_{\text{click}}=1/(\langle\tau_{\text{click}}\rangle+\tau_{\text{dead}})$ , where  $\tau_{\text{dead}}$  is the detector dead time after firing and  $\langle\tau_{\text{click}}\rangle$  is the mean time between detector firing events. For a detector pair in a coincidence heralding scheme, the dead-time-reduced coincidence rate is  $R_{\text{coinc}}=1/[\langle\tau_{\text{click}}\rangle+\tau_{\text{dead0}}/P(\text{coinc}|\text{click0})+\tau_{\text{dead1}}]$ , where  $\tau_{\text{dead0}}$  and  $\tau_{\text{dead1}}$  are the dead times for each detector and  $P(\text{coinc}|\text{click0})$  is the probability of a coincidence (i.e., the probability detector D1 clicks) given that the heralding detector, D0, clicked. For high contrast (low accidentals) coincidences, we have  $R_{\text{coinc}}=1/(\langle\tau_{\text{click}}\rangle+\tau_{\text{dead0}}/\eta_{D1}+\tau_{\text{dead1}})$ .

The ratio of the measured coincidence rate from a correlated-photon source (including both correlated and uncorrelated contributions) to that of an uncorrelated source is

$$\Gamma(\mu)=\frac{P_{\text{coinc}}+P_{\text{acc}}}{P_{\text{acc}}}=1+\frac{\mu}{2(\mu+\mu_{d0})(\mu+\mu_{d1})}, \quad (1)$$

where the detector contribution is completely described by the noise-equivalent-photon probability,  $\mu_{di}=P_{di}/\eta_i$ , a parameter which can also absorb uncorrelated background photons. Improved methods of single photon detection can increase the ratio in (1) and also permit alternate modes of operation, such as heralding.

The experimental setup for heralding detection of correlated photons is shown in Fig. 1 and is similar to those of Refs. 12 and 13. Heralding was accomplished with a SSPD, operated at 4.25 K in a cryogen-free system, by sending one output of the beam splitter in Fig. 1 to the ungated SSPD. The  $I_c$  of the SSPD was measured to be 24  $\mu\text{A}$ , and a bias current  $I_b=14$   $\mu\text{A}$  was applied to the device. To maximize  $\eta$ , typically  $I_b/I_c \sim 1$ . For this experiment, however,  $I_b/I_c \sim 0.6$ , sacrificing the optimum  $\eta$  to maintain a very low  $P_d$ . The SSPD is D0 detector and an InGaAs APD is D1 detector in Fig. 1.

The APD was gated to look for a photon at delay  $\tau_D$  after the SSPD recorded a detection event, with the coincidence

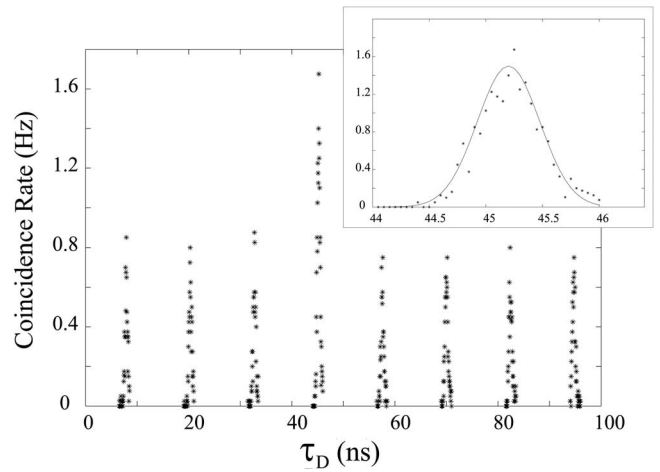


FIG. 2. A plot of the coincidence rate as a function of the delay between SSPD photoresponse and the gating signal of the InGaAs APD. The central peak is larger than the side peaks indicating correlated-photon pair production. The central peak height corresponds to  $P_{\text{coinc}}+P_{\text{acc}}$  and the side peak height corresponds to  $P_{\text{acc}}$  defined in the text. The inset shows a Gaussian fit to a zoom in of the central peak.

event rate as a function of the delay  $\tau_D$  shown in Fig. 2. The graph shows a set of peaks separated by 12.5 ns, the period between consecutive laser pulses. The central peak, located at  $\tau_D \sim 45$  ns, shows an elevated coincidence rate, indicating that for this value of  $\tau_D$  the APD is triggered to detect photons from the same optical pulse as the SSPD and indicating the presence of photon correlations. The excess signal is due to correlated-photon pairs. The peaks in the figure have a finite width that is approximated by a Gaussian distribution to guide the eye (see inset of Fig. 2) with a standard deviation of approximately 350 ps which is commensurate with InGaAs APD photoresponse jitter. The signal in the side peaks is due solely to accidentals, since we assume no correlation between pairs from successive laser pulses. Using standard two-photon detector calibration techniques,<sup>14,15</sup> the data in Fig. 2 are used to calculate the detection efficiencies of the two detectors and the value of  $\mu$ . Deducting the independently measured system losses of  $\eta_{\text{loss}}=10$  dB, the detection efficiencies for the two detectors are  $\eta_{\text{APD}}=10.6\% \pm 1.7\%$  and  $\eta_{\text{SSPD}}=0.065\% \pm 0.014\%$ , with uncertainties based on the  $1-\sigma$  purely statistical variance of the measured efficiencies. The low SSPD detection efficiency was verified with an attenuated laser pulse and is attributed to spatial misalignment at the fiber/SSPD interface combined with the low current bias operating point described above. The calculated value of  $\mu$  increased linearly with pump power, as expected, with a slope of 0.02/mW.

The reduced after pulsing and dead times of SSPDs can facilitate faster measured coincidence rates. The curves in Fig. 3 compare the detection coincidence rate as a function of system clock frequency for three different detector technologies: the InGaAs APD pair measured in this letter, the SSPD/APD pair measured in this letter, and the best reported performance of an SSPD,  $\eta_{\text{SSPD}}=57\%$ , reported in Ref. 9. The APD/APD curve illustrates that for higher clock frequencies, the dead time saturates the coincidence rate, with little improvement possible even for increases in the other operating parameters; higher pair flux  $\mu$ , higher efficiency, and lower losses. For SSPD/APD heralding, substantially higher rates are possible.

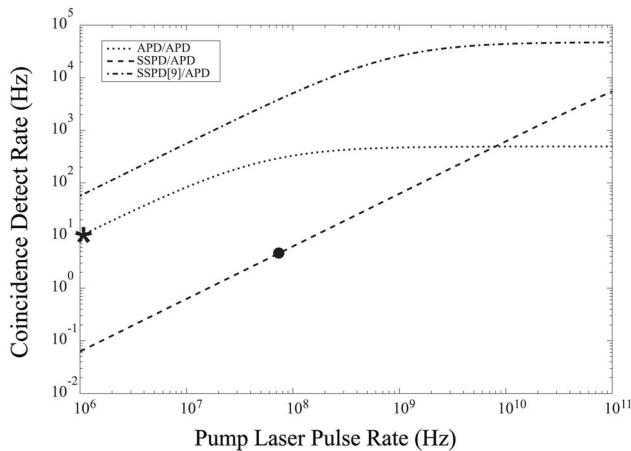


FIG. 3. The detection coincidence rate as a function of system clock frequency for multiple detector technologies. The dotted line is for a pair of measured InGaAs APDs, the dashed curve is for the measured SSPD/APD pair, and the dot-dash curve is for the best reported SSPD characteristics (Ref. 9). Measured coincidence rates for APD/APD clocked operation at 1 MHz (★) and for SSPD/APD heralded operation at 80 MHz (●) are shown.

The measured SSPD/APD coincidence detection rate, marked by a (●) in Fig. 3, on the order of 1/s is slightly smaller than typically measured APD/APD coincidence detection rates of near 5/s, marked by a (★), despite the factor of 150 reduction of detection efficiency between the SSPD and the APD. The SSPD/APD measurement was able to fully exploit the optical pulse rate, 80 times faster than for a pair of APDs clocked at 1 MHz, due to the short SSPD dead time. Even more improvement would be realized for higher laser pulse rates and for cw laser pumping, boosting the coincidence rate dramatically.

Following Eq. (1) the contrast ( $\Gamma$ ) is a function of the pair production rate or pump power. Figure 4 plots the measured contrast as a function of the pump laser power. The data were collected by varying the pump laser power and measuring the coincidence rate at two values of  $\tau_D$  corresponding to the central peak and one side peak with integration period between 10 to 100 s. Also plotted in Fig. 4 is the calculated contrast from Eq. (1) using the efficiencies measured above, and the dark count rates of each detector are measured to be  $P_d(\text{APD})=1.0 \times 10^{-5}$  and  $P_d(\text{SSPD})=2.6 \times 10^{-6}$ . The fit agrees well with the measured contrast ratio of the data over the range of pump power. The measured

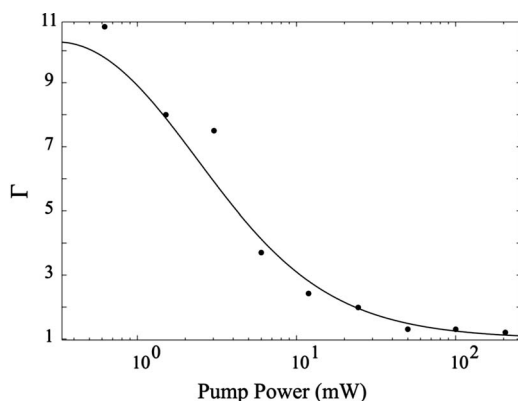


FIG. 4. The dots are measurements of the contrast of the center peak to the side peaks (as shown in Fig. 2) as a function of the power from the pump laser. Equation (1) is plotted as a solid line using the measured parameters from the experiment.

noise-equivalent-photon level for the APD is  $\mu_d(\text{APD})=9.4 \times 10^{-4}$ . The SSPD level is not as good,  $\mu_d(\text{SSPD})=4.0 \times 10^{-2}$ , due to the low detection efficiency.

The experiment presented here demonstrates the proof-of-principle use of a SSPD in a photon pair heralding scheme which can improve detection of coincidence events between two correlated telecommunication wavelength photons. The SSPD is used as an ungated or *staring-mode* detector, sensitive at 1550 nm, to herald the arrival of the 1550 nm twin photon. This staring-mode operation is commonly used with Si APDs in the visible wavelengths and has performance advantage over gated-mode operation, typical of InGaAs APDs, for the detection of photon pair coincidences. SSPD staring-mode operation and faster dead time are leveraged to allow higher clock speeds, demonstrated in this letter at 80 MHz.

The ultimate goal of this project is the development of a fiber-based entangled quantum cryptography link as an addition to the DARPA Quantum Network developed by BBN Technologies.<sup>16</sup> To date, many entangled photon sources have operated by producing correlated photons with different wavelengths, commonly one photon in the visible and one at telecommunication wavelengths, allowing for shared quantum information between a party at the source and a remote party. The source demonstrated here, along with the improved detection, generalizes the scheme allowing two arbitrary, separated parties to share an entangled-photon pair generated from a remote source of entanglement.

This effort was funded by DARPA under the QuIST program Contract No. F20602-01-2-0528 and support from the NIST QI program. The authors thank J. Schlafer from BBN and A. J. Miller and R. E. Schwall from NIST for technical assistance and M. Teich and A. Sergienko at BU for discussions on photon statistics. The use of a trade name does not imply endorsement by NIST.

<sup>1</sup>N. Gisin, G. Ribordy, W. Tittel, and H. Zbinden, Rev. Mod. Phys. **74**, 145 (2002).

<sup>2</sup>C. Elliott, D. Pearson, and G. Troxel, Comput. Commun. Rev. **33**, 227 (2003).

<sup>3</sup>S. Cova, M. Ghioni, A. Lotito, I. Rech, and F. Zappa, J. Mod. Opt. **51**, 1267 (2004).

<sup>4</sup>D. S. Bethune, W. P. Risk, and G. W. Pabst, J. Mod. Opt. **51**, 1359 (2004).

<sup>5</sup>M. A. Albota and E. Dauler, J. Mod. Opt. **51**, 1417 (2004).

<sup>6</sup>B. Cabrera, R. M. Clarke, P. Colling, A. J. Miller, S. Nam, and R. W. Romani, Appl. Phys. Lett. **73**, 735 (1998).

<sup>7</sup>R. H. Hadfield, M. J. Stevens, S. S. Gruber, A. J. Miller, R. E. Schwall, R. P. Mirin, and S. W. Nam, Opt. Express **13**, 10846 (2005).

<sup>8</sup>A. J. Kerman, E. A. Dauler, W. E. Keicher, J. K. W. Yang, K. K. Berggren, G. Gol'tsman, and B. Voronov, Appl. Phys. Lett. **88**, 111116 (2006).

<sup>9</sup>K. M. Rosfjord, J. K. W. Yang, E. A. Dauler, A. J. Kerman, V. Anant, B. M. Voronov, G. N. Gol'tsman, and K. K. Berggren, Opt. Express **14**, 527 (2006).

<sup>10</sup>J. Zhang, W. Stysz, A. Verevkin, O. Okunev, G. Chulkova, A. Korneev, A. Lipatov, G. N. Gol'tsman, and R. Sobolewski, IEEE Trans. Appl. Supercond. **13**, 180 (2003).

<sup>11</sup>A. Verevkin, A. Pearlman, W. Stysz, J. Zhang, M. Currie, A. Korneev, G. Chulkova, O. Okunev, P. Kouminov, K. Smirnov, B. Voronov, G. N. Gol'tsman, and R. Sobolewski, J. Mod. Opt. **51**, 1447 (2004).

<sup>12</sup>S. Fasel, O. Alibert, S. Tanzilli, P. Baldi, A. Beveratos, N. Gisin, and H. Zbinden, New J. Phys. **6**, 1 (2004).

<sup>13</sup>T. Pittman, B. Jacobs, and J. Franson, Opt. Commun. **246**, 545 (2005).

<sup>14</sup>A. N. Penin and A. V. Sergienko, Appl. Opt. **30**, 3582 (1991).

<sup>15</sup>A. Migdall, R. Datla, A. V. Sergienko, J. S. Orszak, and Y. H. Shih, Metrologia **32**, 479 (1996).

<sup>16</sup>C. Elliott, New J. Phys. **4**, 46.1 (2002).

<sup>17</sup>This definition is equivalent to describing  $\mu$  as the probability of a photon pair being generated, but only in the limit of  $\mu \ll 1$ .